Deconvolution and Vertical Seismic Profiles

Ronald F. Ullmann

Abstract

Two methods of deconvolution were tested on vertical seismic profile (VSP) data for the purpose of finding out which method resolves the events on a VSP better. The first method of deconvolution was calculated in the time domain through inverse filters derived through Backus-Gilbert inverse theory. The second method of deconvolution was calculated in the frequency domain by dividing the Fourier transform of the trace by the smoothed Fourier transform of the source waveform. Source waveforms were taken from uphole geophone recordings and from the first break on the traces recorded by the well geophone. Various deconvolutions were done with these two different source waveforms to determine which gave sharper results for the events on the VSP. The following processing steps were found to produce the best deconvolved VSP:

1. Before any gain has been applied to the data, window the traces from the well geophone to separate the first break event from the rest of the data.
2. Find the autocorrelation of the source waveforms obtained in step 1.
3. Average the autocorrelation of each trace with the autocorrelations from neighboring waveforms.
4. Find the Fourier transform of the averaged autocorrelation and smooth it with a short window function in the frequency domain.
5. Find the Fourier transform of the entire trace and divide it by the smoothed function found in step 4.
6. Take the inverse Fourier transform of the results of step 5.

Introduction

Deconvolution is the art of finding the impulse response of the earth from the signal measured by a geophone. Theoretically, this can be done if the source waveform is known. Let $s(t)$ be the time function that is recorded at the surface and $g(t)$ be the impulse response of the earth. A seismic source waveform, $k(t)$, enters the ground at the surface. The output recorded at the surface by the geophone is

$$s(t) = g(t) * k(t)$$

where * is the convolution operator. The problem with this equation is that $k(t)$ is usually not sufficiently impulsive to allow a fine resolution of the reflections. If $k(t)$ were known, then the impulse response of the earth could be found through deconvolution of the output:

$$g(t) = s(t) * \frac{1}{k(t)}$$

Since the seismic waveform, or $k(t)$, is not known for a surface seismic survey, other approaches must used, such as estimating the shape of the wavelet. If the source waveform could be measured or detected directly from the trace from a regular seismic survey, deconvolution would be easier. However, this is not the case and geophysicists must use other sources, such as the vertical seismic profile.

There are two different sources of information about the seismic source for a vertical seismic profile (VSP). The question is which one should be used? Two methods are deconvolution were used on the VSP data. First, I will discuss the two sources of the source waveform. Next, I will discuss the two methods that were used and a fast time shifting operator that was discovered during the work done for this article. Finally I will present the results of the deconvolution.

Finding the Source Waveform

The major difference between a regular seismic survey and a VSP is that the shot waveform is more readily available for a VSP than it is in regular seismic data. When VSPs are recorded, two different geophones are normally used. Figure 1 shows the relative positions of these geophones. The first geophone, which is known as the well geophone, is suspended by a cable and lowered to the bottom of the well. After reaching the bottom, the geophone is raised toward the surface, stopping at specified intervals of about twenty-five to one hundred feet. At each stop, the well geophone is clamped to the side of the well, a seismic waveform is entered at the surface, and a recording of the signal measured by the well geophone is made. The geophone is then raised to the next level. The second

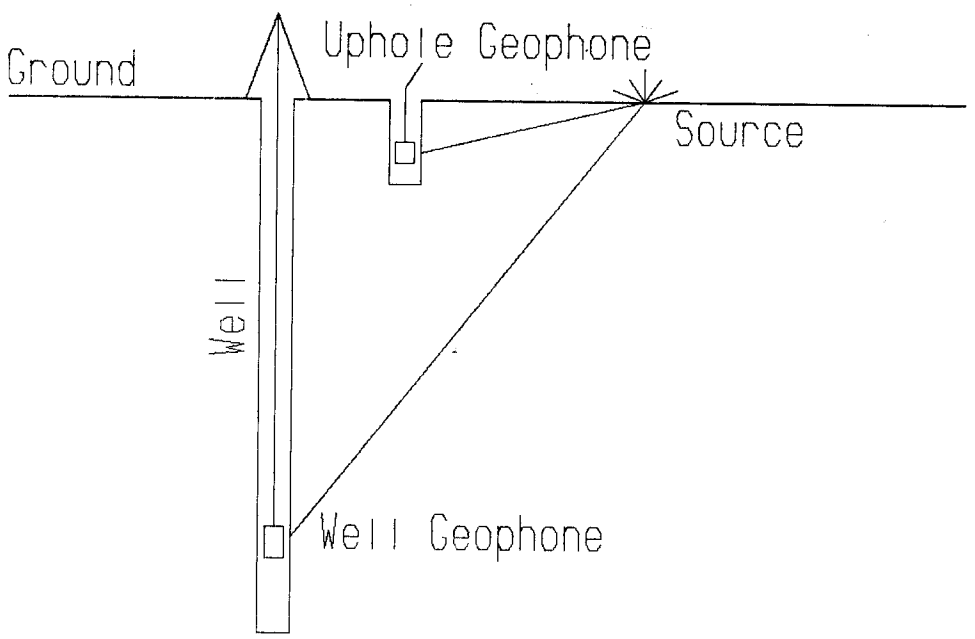

FIG. 1. Location of the geophones during a typical vertical seismic survey. The picture is not drawn to scale.

geophone, known as the uphole geophone, is placed in a shallow hole near the well opening. The uphole geophone also records a signal from the seismic source, but the geophone remains in the hole. Therefore, the uphole geophone can be used to detect differences in the shot waveform since the geophone's position and orientation never varies. The record of the signal detected by the uphole geophone is a recording of the seismic source. This record is not available for surface surveys since the seismic source does not remain in a fixed area for each shot as it does for a VSP. For land seismic surveys, it is too expensive and time consuming to drill a separate hole for a geophone near each shot. In marine seismic work, a hydrophone cannot be dragged along the bottom to record the seismic pulse as it enters the seafloor. Thus, the presence of the uphole geophone in VSP provides valuable information about the source, which can be used in deconvolution.

A second source of the seismic source waveform is the first break on the traces from the well geophone. Figure 2 shows an example of the first breaks for a VSP. The first break is a high amplitude event that marks the arrival of the p-wave. Since this is a direct wave, it arrives at the well geophone before any other type of wave. The first break can be windowed from the section and used to model the source. This wave has the advantage of showing the effects of attenuation on the input waveform as a function of depth. There is no corresponding first break on regular seismic surveys because the first wave direct from

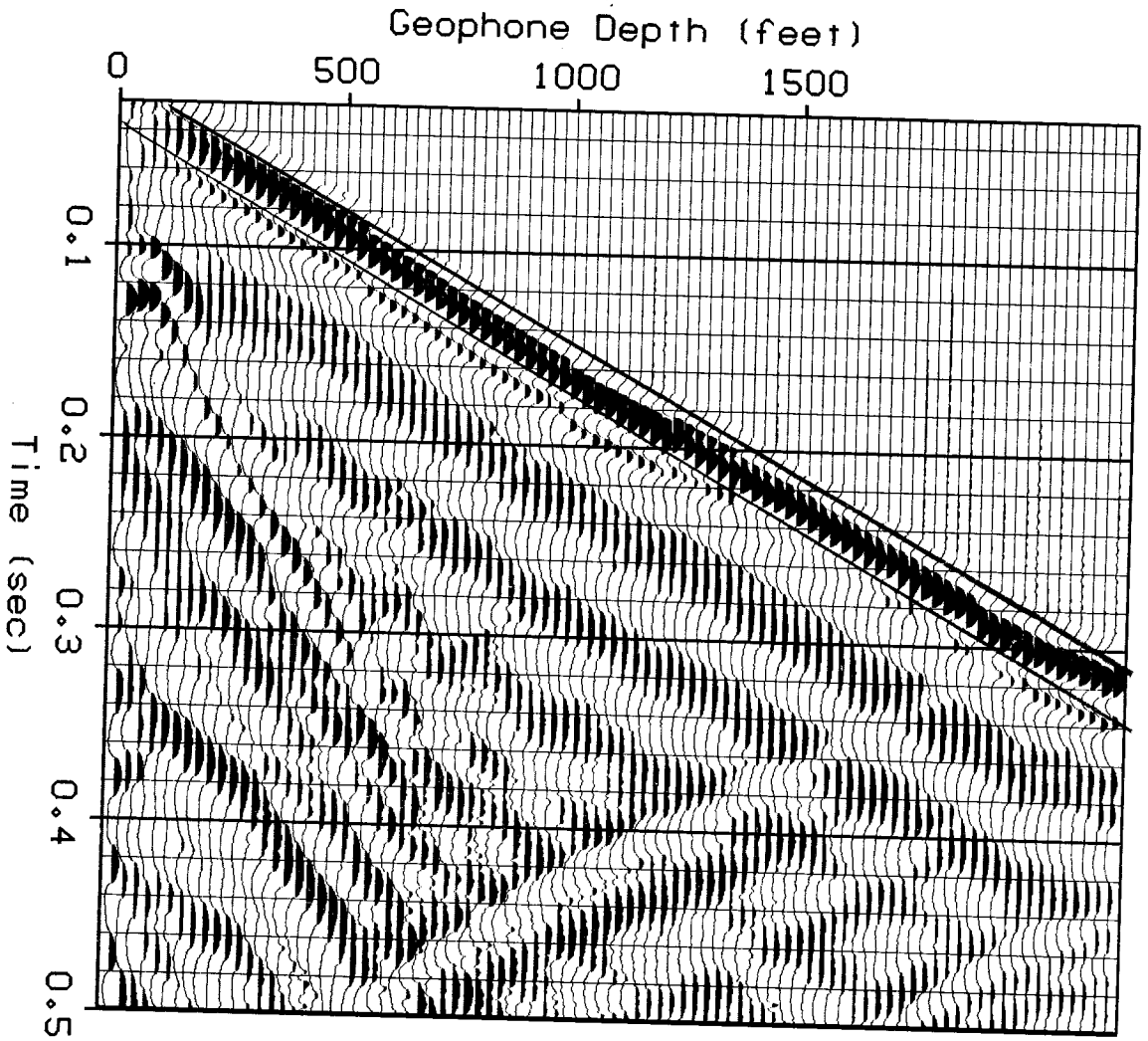

FIG. 2. The original VSP data set before any processing is done. The first break events of the VSP are located between the two diagonal lines.

the shot to the geophone is the surface wave. Any direct p-wave from the shot is obscured by reflected and refracted waves that arrive first.

Time Domain Deconvolution

Two methods of deconvolution were used for this test. One was done in the time domain and the other was done in the frequency domain. The time domain method consisted building a inverse filter using Backus-Gilbert inverse theory as described by Treitel and Lines

(1982). The theory can be expressed in terms of vector and matrix notation. In the following discussion, let the subscripts of the vector elements represent time.

Define the following vectors:

$\mathbf{k} = col\,(k_0, k_1, \cdots, k_m)$ = amplitudes of the source wavelet,

$\mathbf{b} = col\,(b_0, b_1, \cdots, b_n)$ = shaping filer,

$\mathbf{s} = col\,(s_0, s_1, \cdots, s_{m+n})$ = amplitudes of the actual output,

$\mathbf{d} = col\,(d_0, d_1, \cdots, d_{m+n})$ = amplitudes of the desired output, and

$\mathbf{e} = col\,(e_0, e_1, \cdots, e_{m+n}) = \mathbf{d} - \mathbf{s}$ = the error vector.

Define **K** to be the rectangular matrix of size $(m + n + 1)$ by $(n + 1)$

$$\mathbf{K} = \begin{bmatrix} k_0 & 0 & \cdots & 0 \\ k_1 & k_0 & \cdots & \cdot \\ \cdot & k_1 & \cdots & \cdot \\ \cdot & \cdot & \cdots & \cdot \\ \cdot & \cdot & \cdots & 0 \\ k_m & \cdot & \cdots & k_0 \\ 0 & k_m & \cdots & \cdot \\ \cdot & 0 & \cdots & \cdot \\ \cdot & \cdot & \cdots & \cdot \\ \cdot & \cdot & \cdots & k_{m-1} \\ 0 & 0 & \cdots & k_m \end{bmatrix}$$

The convolution for the output, $s(t) = k(t) * b(t)$, then becomes

$$\mathbf{s} = \mathbf{K}\,\mathbf{b}.$$

The object is to calculate the coefficients for the filter **b** in order to minimize the energy in the error vector, which is given by

$$Q = \mathbf{e}^T\,\mathbf{e}$$

where T is the transpose operator. By constraining the coefficients of the filter so that the energy of the filter is constant, the energy in the error vector becomes

$$Q = (\mathbf{d} - \mathbf{K}\,\mathbf{b})^T\,(\mathbf{d} - \mathbf{K}\,\mathbf{b}) + \lambda(\mathbf{b}^T\,\mathbf{b} - c) \qquad (1)$$

where λ is a Lagrange multiplier. Differentiating Q with respect to **b** and setting it equal to zero, the equation for the filter becomes

$$\mathbf{b} = (\mathbf{R} + \lambda\,\mathbf{I})^{-1}\,\mathbf{g} \qquad (2)$$

where **R** is the autocorrelation matrix $\mathbf{K}^T\,\mathbf{K}$, and **g** is the cross correlation vector $\mathbf{K}^T\,\mathbf{d}$. Since $(\mathbf{R} + \lambda\,\mathbf{I})$ is a Toeplitz matrix, it can be solved quickly using the Levinson recursion (see

Robinson and Treitel, 1980).

Treitel and Lines point out that the presence of the additive constant λI in equation (2) can be derived another way by supposing that the input waveform **k** has some uncorrelated white noise **n** added to it. They assume that the white noise has a mean of zero and a variance of σ_0^2. Define the rectangular matrix **E** to have the same form as **K** above, but in terms of the white noise vector **n** instead of the input waveform vector **k**. Using the constraint that the filter energy be constant, the equation for the energy in the error vector becomes

$$Q = \mathbf{d}^T \mathbf{d} - 2\mathbf{d}^T (\mathbf{K} + \mathbf{E})\, \mathbf{b} + \mathbf{b}^T (\mathbf{K}^T + \mathbf{E}^T)(\mathbf{K} + \mathbf{E})\, \mathbf{b} + \lambda (\mathbf{b}^T \mathbf{E}^T \mathbf{E}\, \mathbf{b} - c) . \qquad (3)$$

Since **n** is white noise, it is uncorrelated with the input **k** and the desired output **d**. Thus equation (3) becomes

$$Q = \mathbf{d}^T \mathbf{d} - 2\mathbf{d}^T \mathbf{K}\, \mathbf{b} + \mathbf{b}^T (\mathbf{K}^T \mathbf{K} + \sigma_0^2 \mathbf{I})\, \mathbf{b} + \lambda (\mathbf{b}^T \sigma_0^2 \mathbf{I}\, \mathbf{b}) .$$

Differentiating Q with respect to **b** and setting it equal to zero, the equation for the filter becomes

$$\mathbf{b} = \left[\mathbf{R} + (1 + \lambda)\, \sigma_0^2 \mathbf{I}\right]^{-1} \mathbf{g} . \qquad (4)$$

Equation (4) has the same form as equation (2), which means that adding white noise to the input signal, results in a more stable filter that can handle the presence of white noise. The positive real constant that is added to the main diagonal of the autocorrelation matrix **R** is to the pre-whitening parameter. By adding this constant, white noise is added to the input signal **k**. Since white noise is uncorrelated with itself, then it only affects the main diagonal of the autocorrelation matrix because these values correspond the zero-lag autocorrelation value of **k**.

The autocorrelations of the source waveforms can be averaged over several traces. For example, the five autocorrelation matrices for traces twenty-eight through thirty-two are calculated and averaged together to form the autocorrelation matrix for trace thirty. A Hanning weighting function was used in the results for this article to weight the autocorrelations matrices surrounding the central matrix. In the example, the weighting function insured that the autocorrelation values for trace thirty had a more significant affect on the average than any other single trace. Averaging eliminates abrupt horizontal changes in the filter caused by sudden differences in the input waveform. Abrupt changes in the source waveform can occur when the source is moved at the surface. These changes occurred several times during the survey that is used here. The filters derived after averaging were more uniform and less affected by noise. Deconvolution in the time domain introduced too

much high frequency noise to the output, as will be seen in the later in the results.

Frequency Domain Deconvolution

A second method deconvolution was done in the frequency domain, an method suggested by Jon Claerbout. This method takes advantage of the fast Fourier transform and therefore takes less computing time. The source waveform, $k(t)$, is Fourier transformed to become $K(\omega)$. A smoothing operator, $H(\omega)$, is applied to $K(\omega)$ to eliminate any unusual irregularities and remove zero amplitude frequency components. Here, a five point Hanning window was used as the smoothing operator for in the frequency domain. This smoothing in the frequency domain corresponds to multiplying the source waveform by a broad window in the time domain. The trace, $p(t)$, was then Fourier transformed to become $P(\omega)$, divided by the smoothed spectra, $(H(\omega) * K(\omega))$, and inversed Fourier transformed. This whole process can be expressed by the equation

$$c(t) = F^{-1}\left[\frac{P(\omega)}{K(\omega) * H(\omega)}\right] \tag{5}$$

where
$c(t)$ is the deconvolved data, and
$F^{-1}[\ ]$ is the inverse Fourier transform.

Variations of this method were tried to determine their effectiveness in deconvolution. These variations consisted of substituting other functions for the denominator in equation (5). The first variation used the Fourier transform of the trace $P(\omega)$ instead of $K(\omega)$. The equation for this operation is

$$c(t) = F^{-1}\left[\frac{P(\omega)}{P(\omega) * H(\omega)}\right] \tag{6}$$

The second variation was to use the amplitude spectrum of the source waveform. This is equivalent to using the autocorrelation of the source waveform. This test was done see how a zero phase waveform would affect the deconvolution. The equation for this operation is

$$c(t) = F^{-1}\left[\frac{P(\omega)}{(K(\omega)\,\overline{K(\omega)}) * H(\omega)}\right]$$

where $\overline{K(\omega)}$ is the complex conjugate of $K(\omega)$.

The third variation was to use the amplitude spectrum of the trace. The equation for this operation is

$$c(t) = F^{-1}\left[\frac{P(\omega)}{(P(\omega)\,\overline{P(\omega)}) * H(\omega)}\right].$$

The fourth variation was to average the source waveforms with surrounding waveforms before finding its Fourier transform. The averaging was done to remove the effect of variations in the source waveform. A five point Hanning window was used to smooth the adjacent waveforms. The equation is

$$c(t) = F^{-1}\left[\frac{P(\omega)}{F\,[\,h(x) * k(x,t)\,] * H(\omega)}\right]$$

or

$$c(t) = F^{-1}\left[\frac{P(\omega)}{(H(k_x)\,K(k_x,\omega)) * H(\omega)}\right]$$

where

x is the dimension that corresponds to the depth of the well geophone,

$h(x)$ is the smoothing operator over the different waveforms,

$k(x,t)$ are the source waveforms,

$H(k_x)$ is the Fourier transform of the smoothing operator over the different waveforms, and

$K(k_x, \omega)$ is the two dimensional Fourier transform of the source waveforms.

The fifth variation involves combinations of the variations above. The autocorrelation of the waveform was calculated and then averaged with autocorrelations of nearby waveforms. The Fourier transform of the averages were found, smoothed, and used in the denominator. The equation for this operation is

$$c(t) = F^{-1}\left[\frac{P(\omega)}{(K(k_x, \omega)\,\overline{K(k_x, \omega)}\,H(k_x)) * H(\omega)}\right].$$

A Quick Time Shifting Operation

The first variation, which is described by equation (6), may appear to be an identity operation, in that no change would occur to the data. However, the actual results of this operation were surprising. When this process was applied to the data shown in figure 2, it resulted in the time shifted VSP shown in figure 3. The traces were shifted so that the first break event of each trace was lined up in a horizontal line along the top of the section. The reason equation (6) produces this result can be explained intuitively. First, the process started with raw data, which did not have any gain applied to it. Without the gain, the first break event of each trace has a much larger amplitude than the rest of the signal. Figure 4

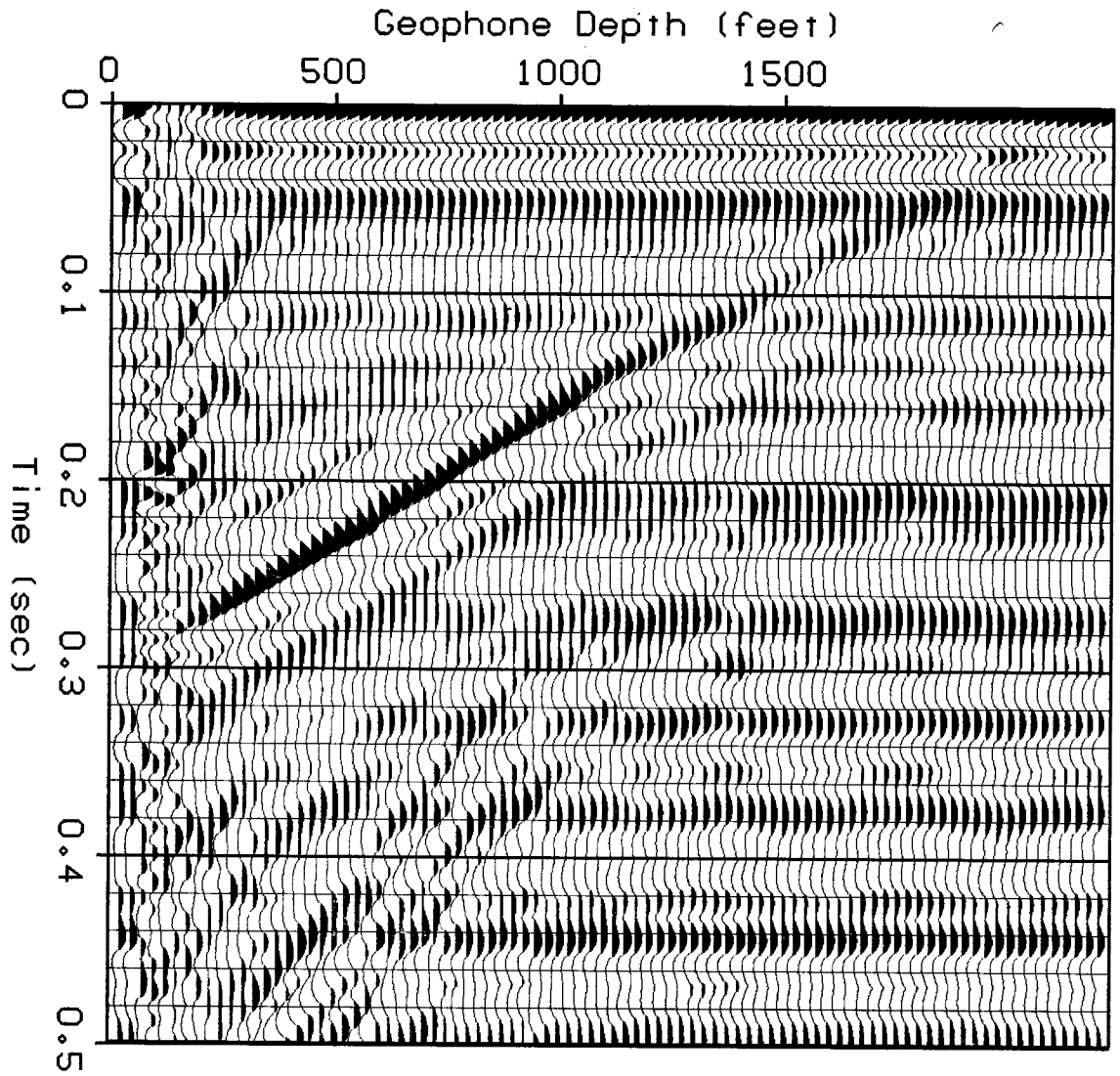

FIG. 3. Time shifted VSP. The traces have been shifted so that the first break event lines up along the top of the section.

shows the amplitudes of a typical trace from the data set. The first break resembles an impulsive event due to its sudden large amplitude. Any smoothing done in the frequency domain further accents the impulsive nature of the first break. As the trace from the geophone is deconvolved by this wave, the first break acts as a time shifted impulse function. In other words, the trace is deconvolved by an approximate time shifted impulse function, which shifts the trace. This explanation becomes clearer when expressed in mathematical terms. Let t_0 be the time when the first break occurs. Then the windowed input function can be approximated by a shifted impulse function:

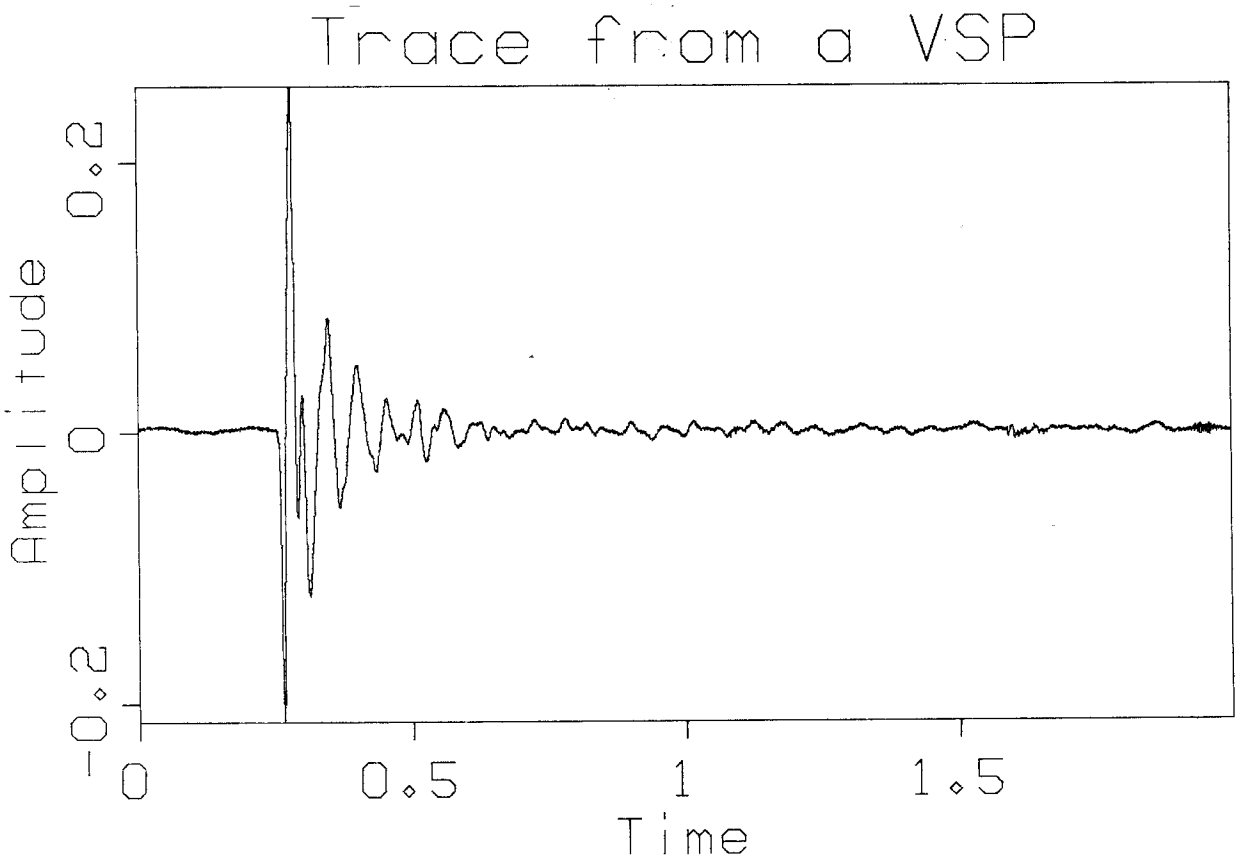

FIG. 4. A typical trace as recorded by the well geophone. No gain has been applied.

$$\delta(t - t_0) \approx p(t)\, h(t)\,,$$

where $p(t)$ is the trace and $h(t)$ is the Fourier transform of the smoothing function. The deconvolved results are

$$c(t) \approx p(t) * \frac{1}{\delta(t - t_0)},$$

which becomes

$$c(t) \approx p(t + t_0)\,.$$

The function, $c(t)$, has a very high amplitude event at $t = 0$. When automatic gain control is applied after the deconvolution, the events after $t = 0$ become apparent, as seen in figure 3.

This operation provides a quick method of shifting the traces in the frequency domain without needing the shift times. The result, though, is not a completely accurate time shift operator because there is some distortion of the shape of the events. This process works

for VSPs due to the strong amplitude of the first break event. As the first break approaches an impulse function, this operation will work better and have less distortion on the signal.

To summarize this process, the steps are:

1. Take the record of a trace from the geophone before any gain is applied and make two copies of it.
2. Multiply one copy by a long window that attenuates the signal except for the area around the first break.
3. Find the Fourier transform of the windowed trace and the untouched trace.
4. Divide the Fourier transform of untouched trace by the Fourier transform of the windowed trace.
5. Take the inverse Fourier transform of this result and apply automatic gain control to it.

The result of the above steps is an approximate time shifted version of the original data.

Obtaining the Source Waveforms

Both locations of the source waveform were used to deconvolve the data. The graph in figure 5 shows a comparison of the two waveforms. The length of the each waveform differs due to the differences in the length of the window that was used to obtain them. The uphole waveform, which is the longer signal, remained free of interference from other events longer than the first break waveform did for the well geophone. The uphole waveform does not come from the p-wave detector of the uphole geophone due to the relative positions of the geophone and source. As can be see in figure 1, a p-wave from the source arrives at the uphole geophone from the side. Since the geophone is oriented vertically, the wave does not excite the p-wave detector of the geophone, but excites one of the s-wave detectors of the geophone. The same problem occurs to the well geophone when it is close to the surface. Most of the plots in this article show incoherent traces in the first few traces. These are due the well geophone no longer picking up the p-wave as effectively. Instead, the p-wave detector was measuring more of the s-wave component of the incoming waves. This causes distortion of the waveform in the trace. A combination of the output from the p-wave detector and the s-wave detector of the well geophone must be used when the geophone is at shallow depths. The first break p-waves used in this article were windowed straight from trace. The diagonal lines in figure 2 show the limits of the window that was used. No attempt was used to incorporate the s-wave components.

Figure 5 shows that the uphole waveform has more high frequencies than the well waveform. This is due to shorter path that the uphole waveform takes to reach the

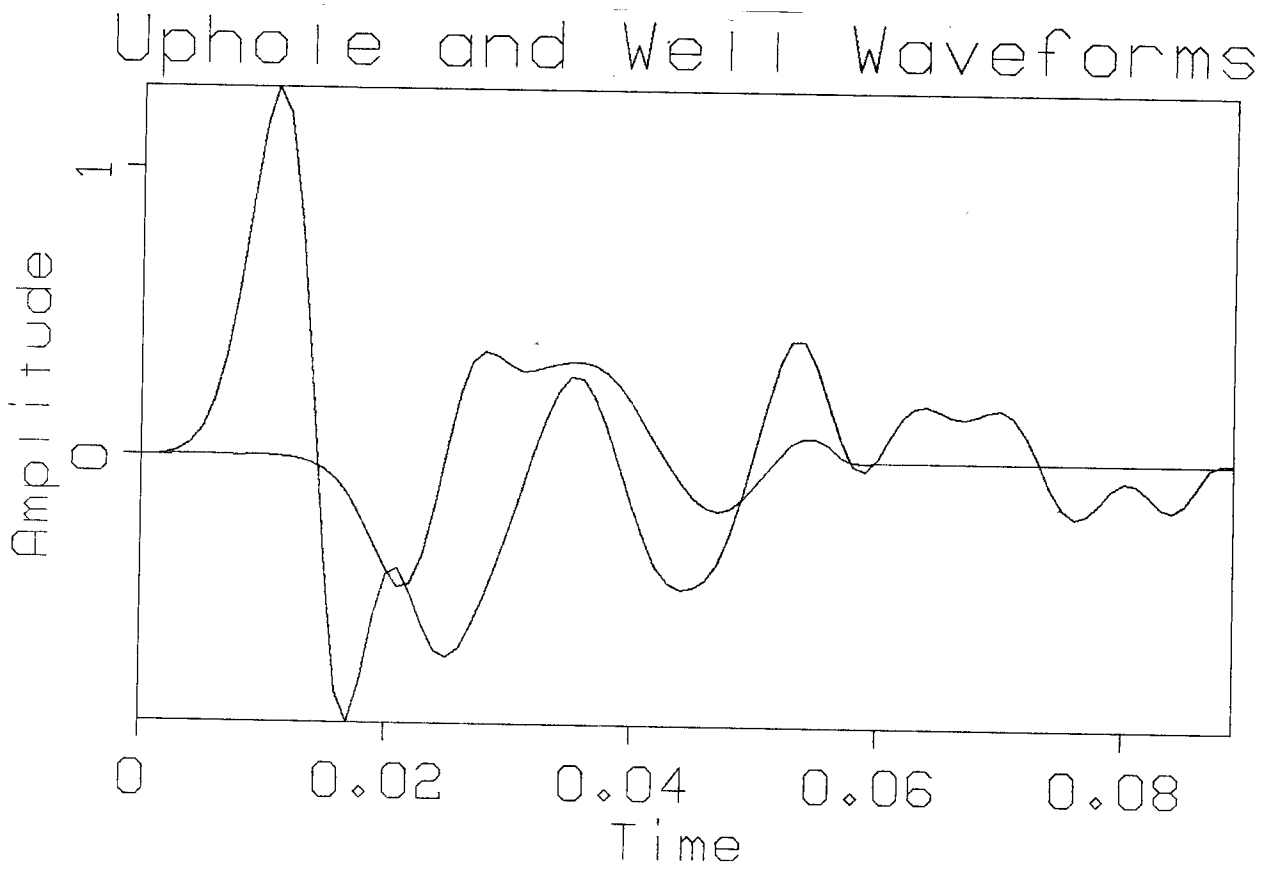

FIG. 5. The source waveforms from the uphole geophone and the well geophone. The wave with the larger amplitude corresponds to the uphole geophone and the smaller to the well geophone.

geophone. As the well geophone moves down, the waveform loses much of its of high frequency due to attenuation. By implication, any deconvolution using the well waveforms will develop more high frequency noise than the uphole waveform because there is less signal in the source waveform at the high frequencies.

Results of the Time Domain Deconvolution Method

The time domain deconvolution results for both source waveforms had a great deal of high frequency noise present in the trace. The data in figure 6 was deconvolved in the time domain using the uphole waveforms as the source waveform. Automatic gain control was applied to the result before plotting to make the plot more understandable. The performances of the inverse filters varied greatly from trace to trace, which resulted in some missing traces. There is also too much high frequency to see any type of event, except for some of the first break event. No improvement in the results was made when the

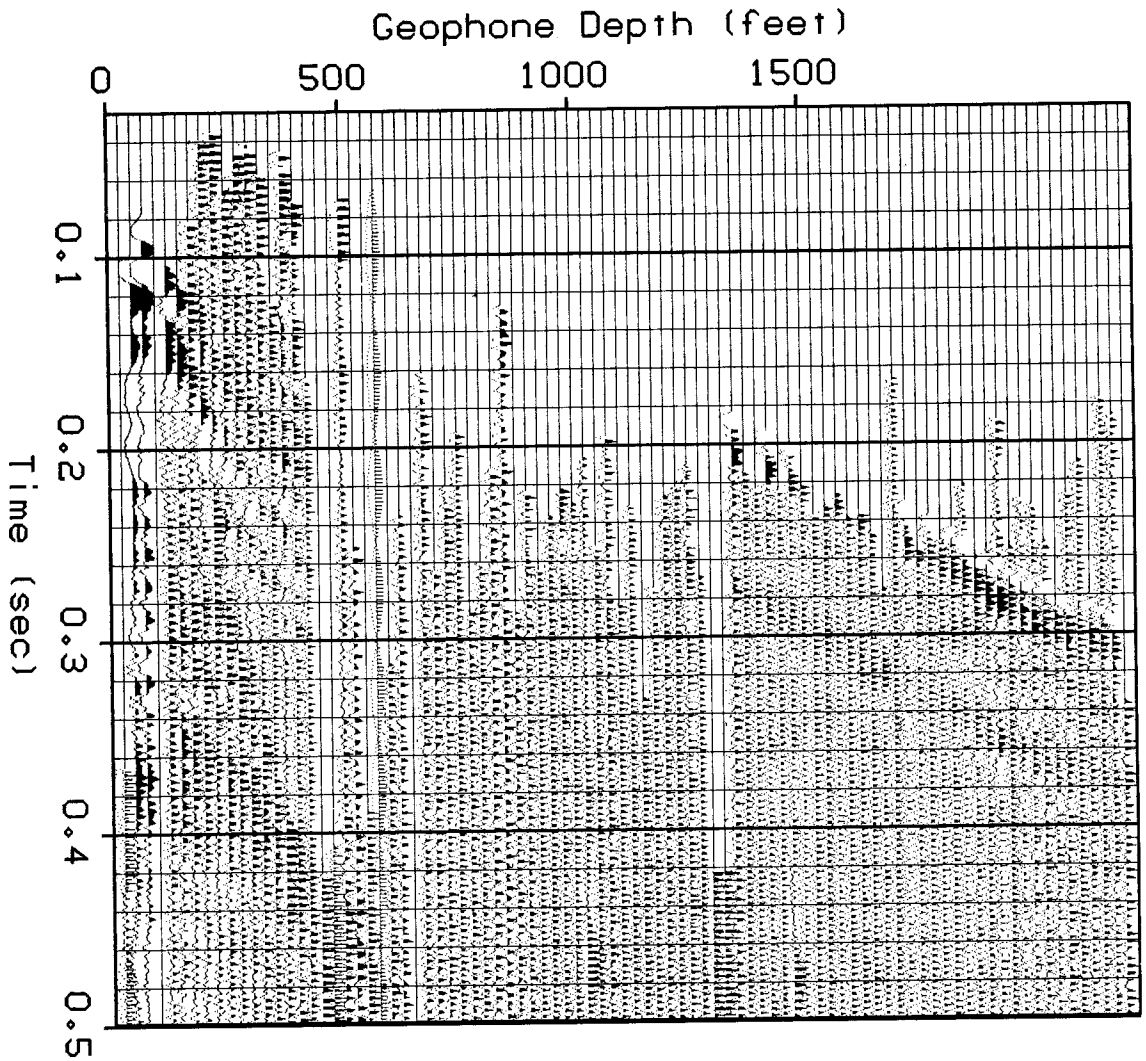

FIG. 6. The VSP data after it was deconvolved in the time domain by the uphole waveform.

deconvolution using the well waveform was performed. In order to see any coherent event on the results from these two deconvolutions, the deconvolved data has to be filtered to remove the high frequencies. Figure 7 shows the same data as figure 6, but after going through a lowpass filter. The downgoing and ungoing events are much more visible in this plot. Figure 8 shows a plot of the filtered results from a time domain deconvolution using the well waveform. A comparison of figures 7 and 8 shows that the deconvolution using the well waveform did a better job across the entire section. The reasons for this judgement are that the upgoing and downgoing events are more evident, the filter performance is more uniform over the different traces, and there are fewer traces without any data.

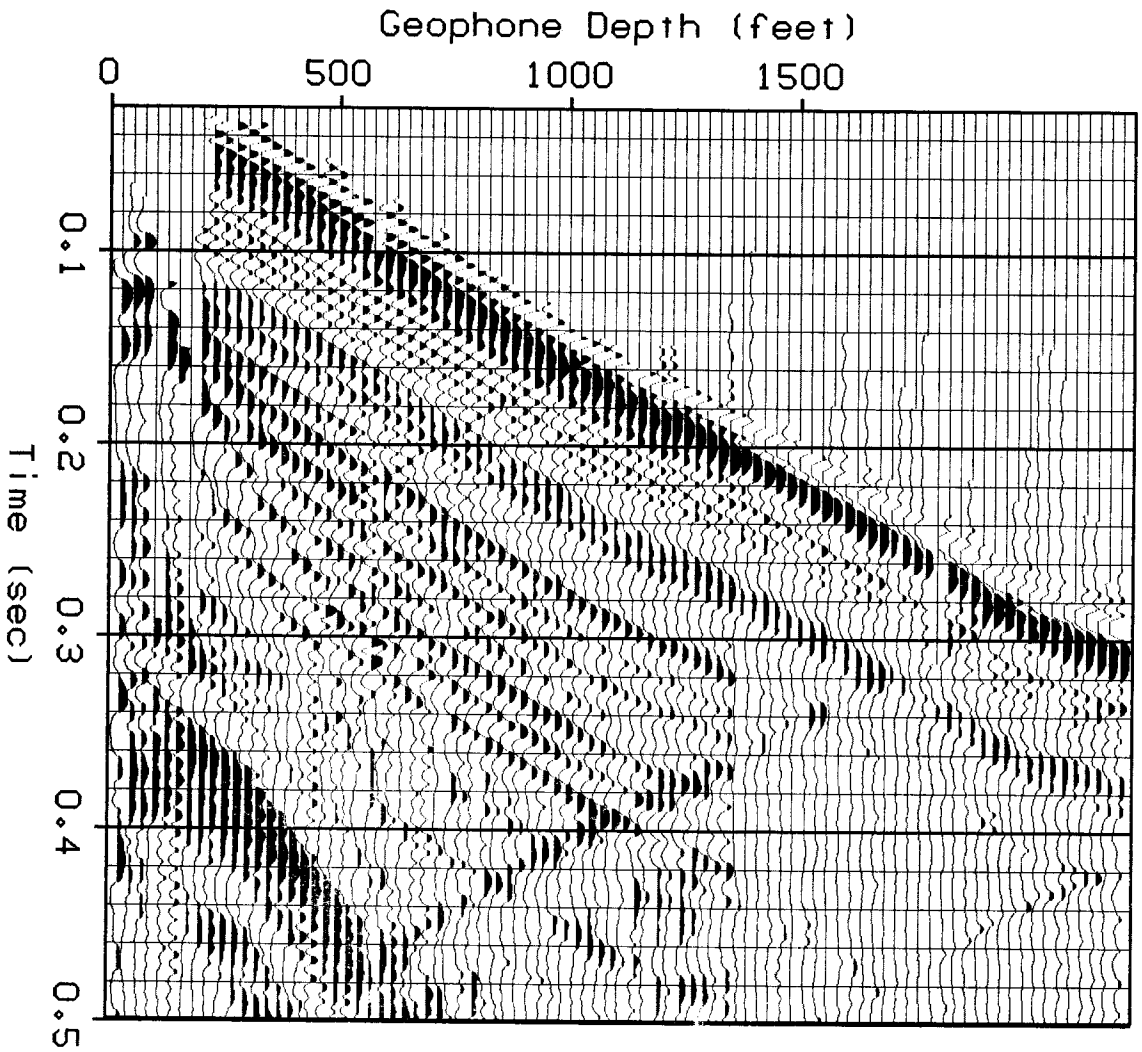

FIG. 7. A filtered version of the data shown in figure 6. This is the VSP data after it has been deconvolved in the time domain by the uphole waveform.

Examination of figures 7 and 8 does show that there are traces that have very little data on them. These dead traces mark traces where the inverse filter failed to have a high performance level. If the autocorrelation of the source waveforms were averaged before the filter was calculated in equation (4), then the dead traces are eliminated. Figure 9 shows the results of deconvolution when the autocorrelation matrices of the well waveform were averaged before the filter was found. The major difference between the results in figures 8 and 9 is that there are no dead traces. Otherwise, there is very little visible difference in the events between the two plots.

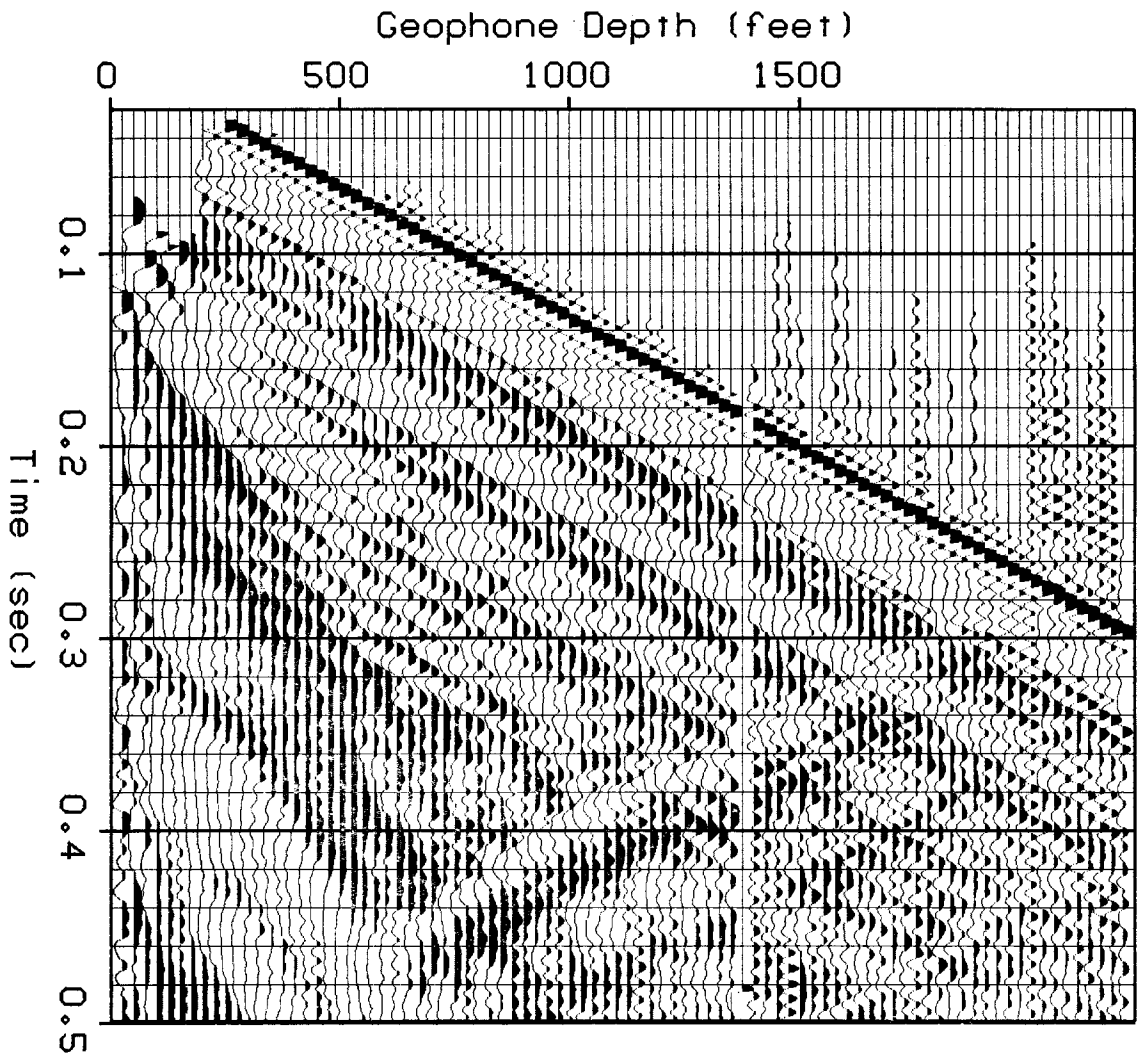

FIG. 8. A filtered version of the VSP data after it has been deconvolved in the time domain by the well waveform.

Results of the Frequency Domain Deconvolution

The time domain method requires post deconvolution low pass filter before the events can be seen. For frequency domain deconvolution, no post deconvolution filtering is required to examine the results. Figure 10 shows the results of a frequency domain convolution using the uphole waveform as the source waveform. There are more high frequencies present than in the original data, but the amplitude of the high frequencies is not as large as for the time domain deconvolution results. The shallow upgoing events, which slope downward from right to left, stand out much more on this section. As a result, it is easier to follow

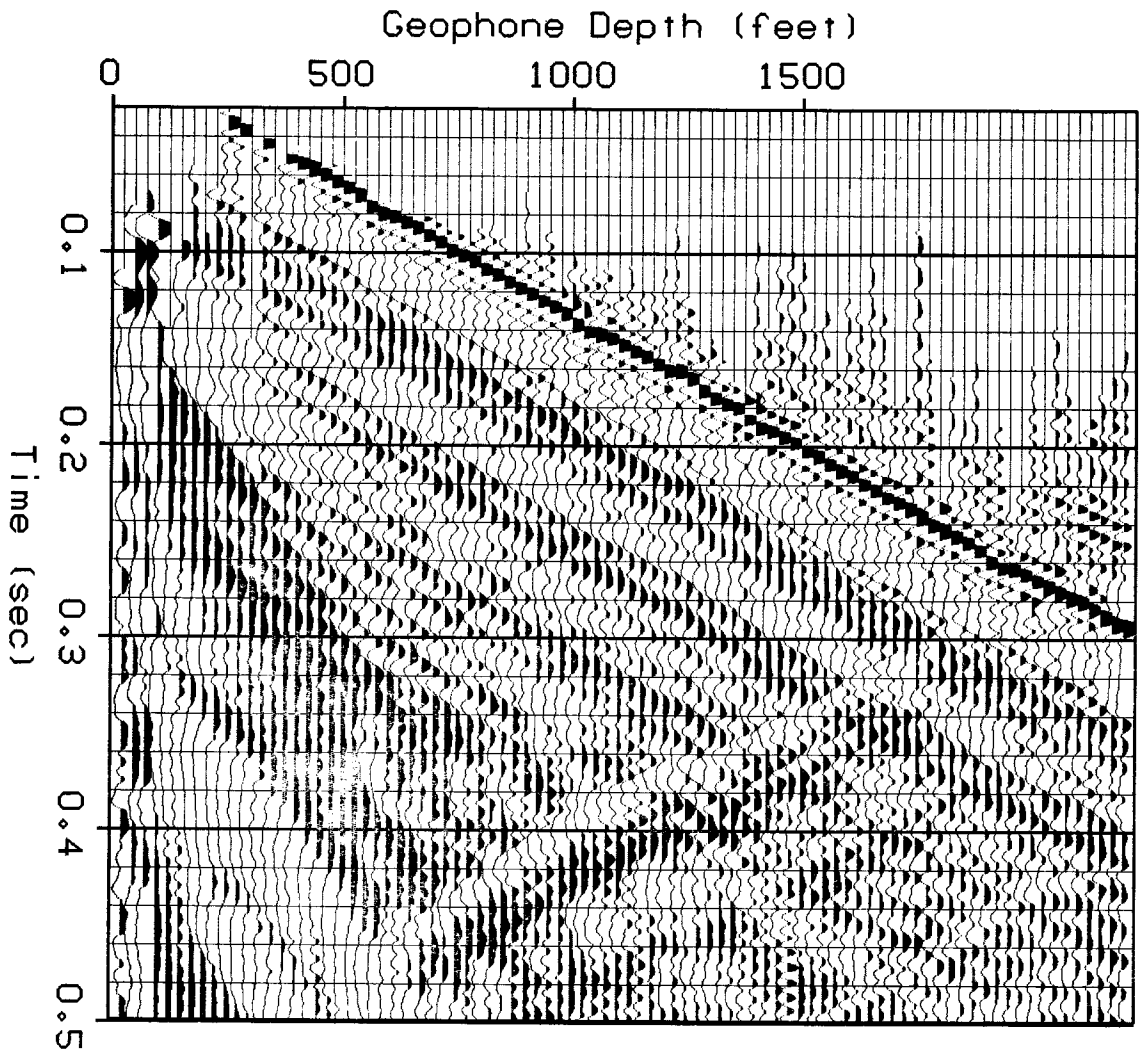

FIG. 9. This plot shows the results when the autocorrelation matrices of the source waveforms are averaged before the filter is found. The source waveform for this plot came from the well geophone.

these events to their intersection with the first break event at the top. Figure 11 shows the frequency domain deconvolution when the well waveform was used as the source. The upgoing and downgoing events are not as sharp, and the downgoing waves tend to obscure the upgoing waves.

All of the variations mentioned in the section covering frequency domain deconvolution were also tried using both the well and uphole waveforms. The results of most of these trials did not produce any results that give better results than in figures 10 and 11. The

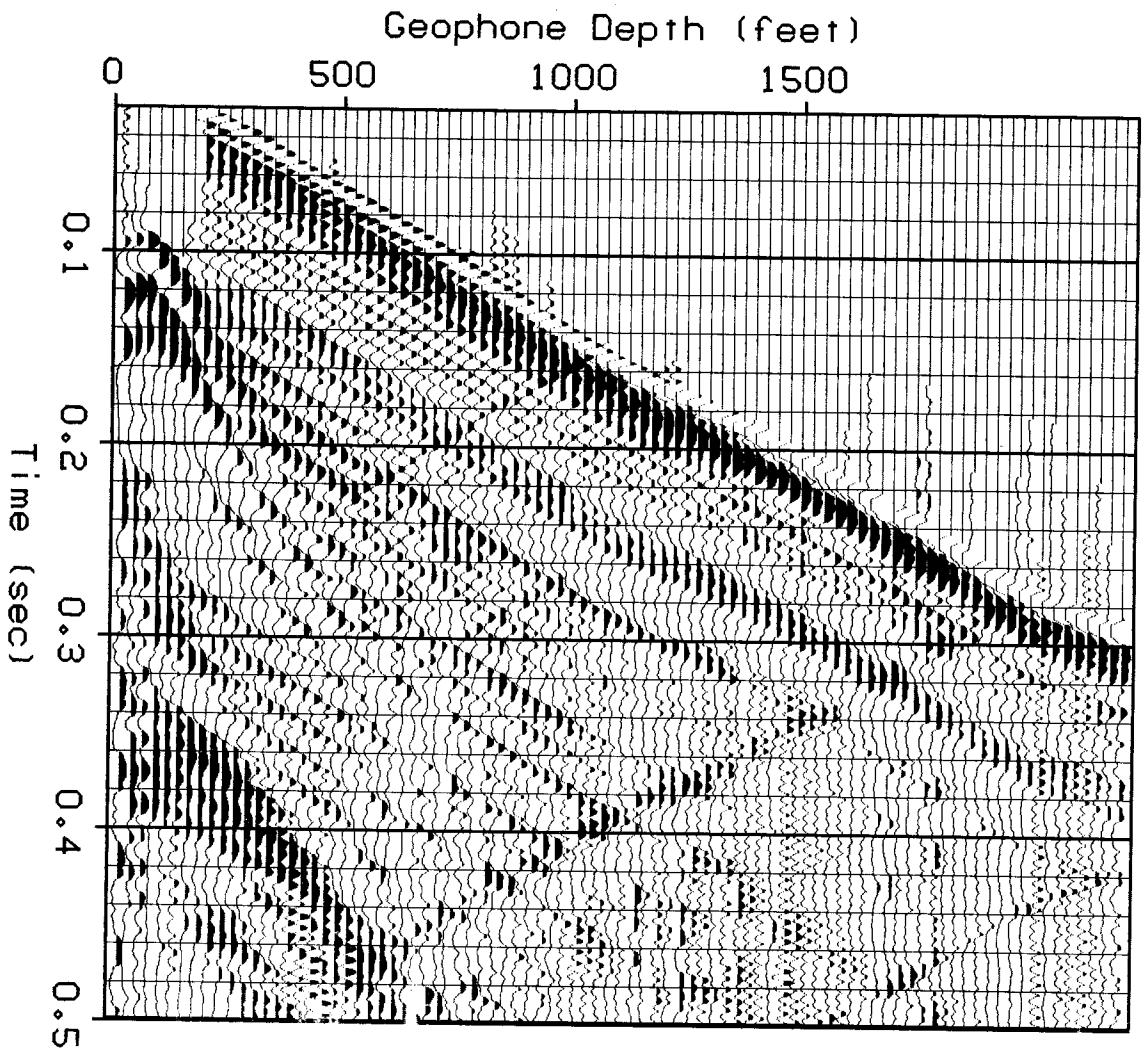

FIG. 10. This plot shows the results of deconvolution in the frequency domain using the source waveform from the uphole geophone.

exception occurred for the fifth variation, where the autocorrelations of the well waveform were calculated and averaged together before taking the Fourier transform. The autocorrelations from the different waveforms were averaged in the same manner that is described in the time domain deconvolution section. Figure 12 shows a plot of the results. There is more high frequency noise present, but not as much noise as there was in figure 10. Also less trace-to-trace variation occurs in the performance of the deconvolution. The significant events on the section are shaper and easier to follow, especially the upgoing events. Of the three figures shown in this section, figure 12 shows the best results.

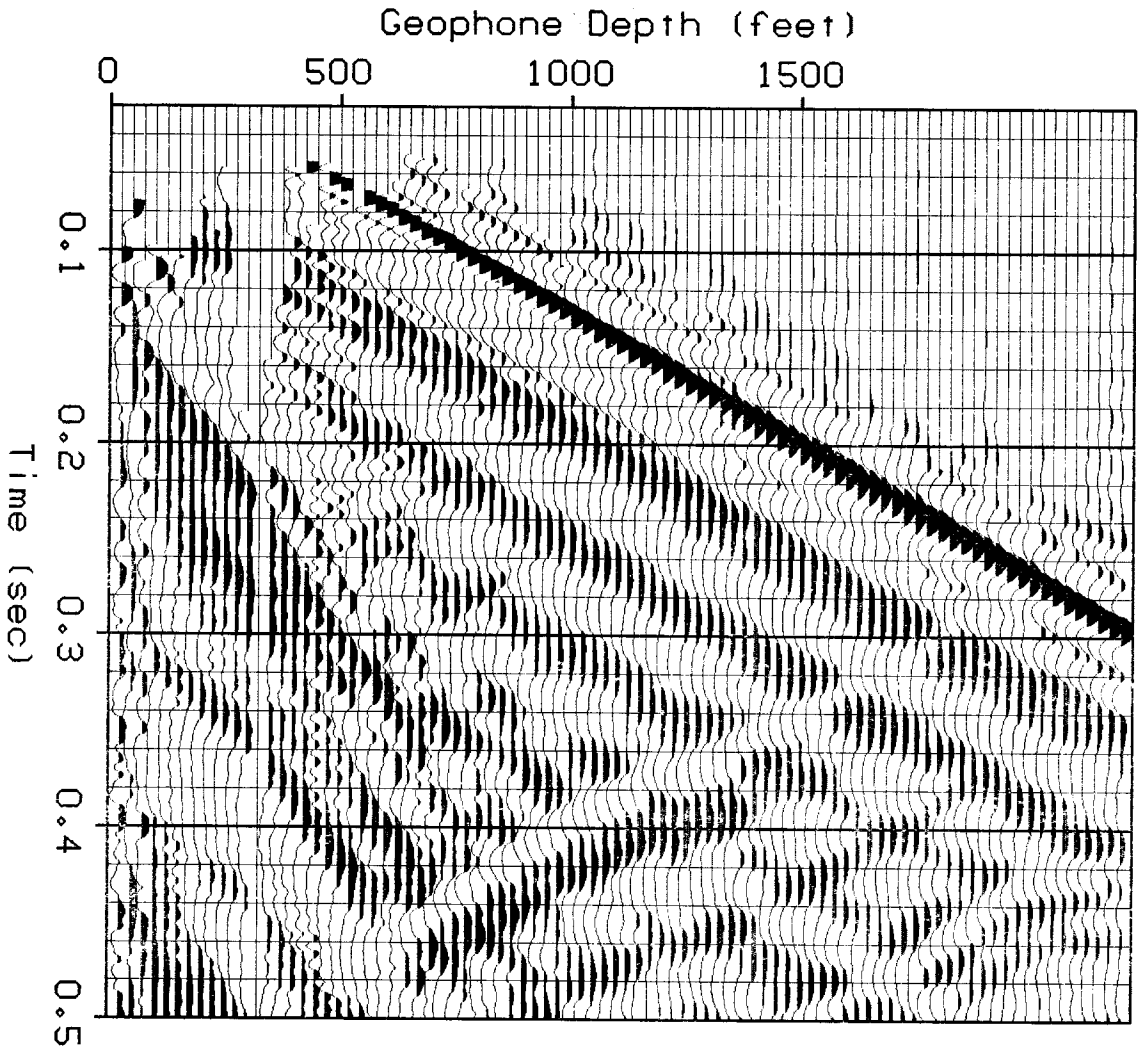

FIG. 11. This plot shows the results of deconvolution in the frequency domain using the source waveform from the well geophone.

Conclusions

After comparing the results of the different methods of deconvolution, the method that produce the better image with less noise is shown in figure 12. The steps for this process are:

1. Window the traces from the well geophone to separate the first break event from the rest of the data. The data for figure 12 did not have any gain applied to it before the processing started. Gain was applied just before plotting the results.
2. Find the autocorrelation of the source waveforms obtained in step 1.

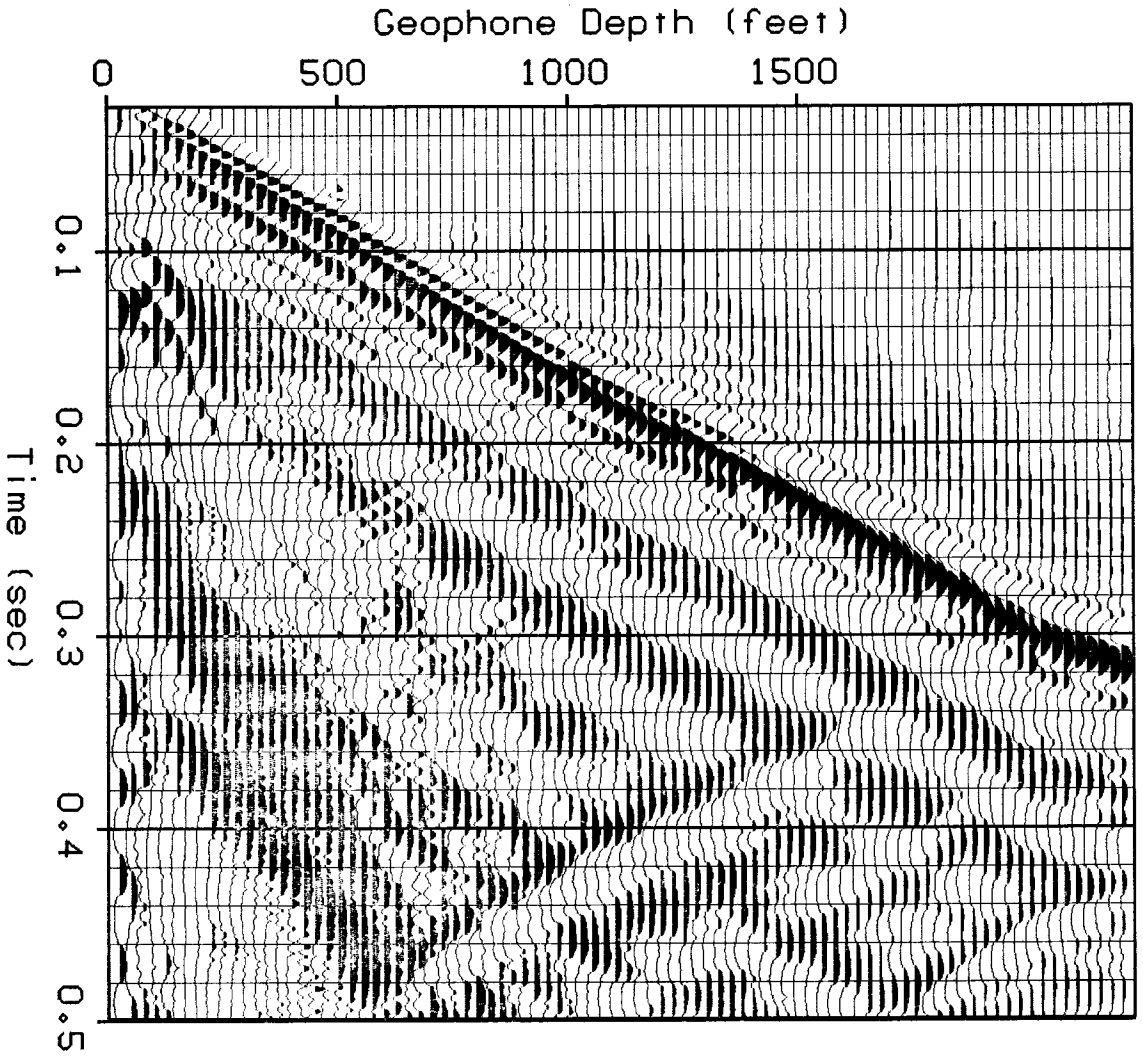

FIG. 12. This plot shows the results of deconvolution in the frequency domain when the averaged autocorrelation of the waveform from the well geophone is used.

3. Average the autocorrelation of each trace with the autocorrelations from neighboring waveforms. A five point Hanning window was used to weight the nearby autocorrelations before they were summed for an average for this article.

4. Find the Fourier transform of the averaged autocorrelation and smooth it in the frequency domain. A five point Hanning window was also used for this in this article.

5. Find the Fourier transform of the entire trace and divide it by the smoothed function found in step 4.

6. Take the inverse Fourier transform of the results of step 5.

The fast Fourier transform makes this deconvolution very fast and easy to do. Based on the results shown in figure 12, this process is not easily affected by sudden changes in the waveform or by a great deal of noise present in the waveform. Some excess high frequency may be present, but a simple filter could be used to eliminate that.

The results of this article does prove that time domain deconvolution is worthless. By using the right post deconvolution filter, the unwanted frequencies added by the deconvolution can be removed, producing a clear section Perhaps some better assumptions about the nature of geophysical data will produce an algorithm that produces more sophisticated inverse filters. For example, a main assumption is that any noise in the signal is white and additive to the source waveform. Further examination of these assumptions is required before time domain deconvolution becomes more useful. There are also other methods of deconvolution in the time domain, such as lattice filter, that need to be explored. Deconvolution of vertical seismic profiles should become a standard operation because information is available about the source waveform.

ACKNOWLEDGMENTS

I want to thank ARCO for the vertical seismic data that was used in this report.

REFERENCES

Robinson, E.A., and Treitel, S., 1980, Geophysical signal analysis: Englewood Cliffs, NJ, Prentice-Hall Inc.

Treitel, S., and Lines, L.R., 1982, Linear inverse theory and deconvolution: Geophysics, v. 47, p. 1153-1159.